Int. J. Electrochem. Sci., 14 **(2019)** 6168 – 6178, doi: 10.20964/2019.07.63

International Journal of ELECTROCHEMICAL SCIENCE
www.electrochemsci.org

Electrochemical Determination of Acebutolol on the Electrochemically Pretreated Screen Printed Carbon Electrode

Annamalai Yamuna[1], Periyasamy Sundaresan[1], Shen-Ming Chen[1,], Shaban R. M. Sayed[2], Tse-Wei Chen[1,3], Syang-Peng Rwei[3,4], Xiaoheng Liu[5,*]*

[1] Department of Chemical Engineering and Biotechnology, National Taipei University of Technology, Taipei 106, Taiwan.
[2]Electron Microscope Unit, Central Laboratory, College of Science, King Saud University, P.O. Box 2455, Riyadh 11451, Saudi Arabia
[3] Research and Development Center for Smart Textile Technology, National Taipei University of Technology, Taipei 106, Taiwan, ROC
[4] Institute of Organic and Polymeric Materials, National Taipei University of Technology, Taipei 106, Taiwan, ROC
[5] Key Laboratory of Education Ministry for Soft Chemistry and Functional Materials, Nanjing University of Science and Technology, Nanjing 210094, China.
[*]E-mail: smchen78@ms15.hinet.net (Shen-Ming Chen), xhliu@mail.njust.edu.cn (Xiaoheng Liu)

Received: 9 March 2019 / *Accepted:* 18 May 2019 / *Published:* 10 June 2019

This work reports the electrochemical determination of acebutolol (ACE) by the screen printed carbon electrode (SPCE). Before the determination, the SPCE was activated by the electrochemical pretreatment. This pretreatment creates the edge plane active sites on the SPCE surface and also it creates the electrochemically active functional groups. The activation process was confirmed by the Raman, SEM and electrochemical analysis. The activated SPCE (aSPCE) revealed the better electrochemical performance when compared with SPCE. It is presumed that, this remarkable performance was obtained from the edge plane active sites and the electrochemically active functional groups (such as carbonyl groups and hydroxyl groups). Further, this aSPCE utilized to the ACE determination in phosphate buffer solutions which received a great significance of analytical performances. It revealed the good sensitivity (1.02 µA μM^{-1} cm^{-2}), linear range (0.01 to 200 µM) and low LOD (0.006 µM). Moreover, it shows significant anti-interference properties in suspected interfering compounds.

Keywords: Edge plane; polymer inks; beta blocker; heart disease; carbonyl groups and basal plane.

1. INTRODUCTION

Increasing industrial pollutants, medical wastes, ecological issues induce the research on the onsite monitoring. So far, several materials were established for the on-site monitoring of clinical,

environmental, biological pollutants [1]. Carbon based electrodes are smart for sensing applications. In particular, screen printed carbon electrodes (SPCE) employed the wide range of applications in sensor field due to their versatility, robustness and low cost [2]. However, the commercial SPCEs are electrochemically inert because they are prepared by the printing and firing the various inks onto the substrates. These inks are generally made by the various ratios of graphite, activated carbons, polymeric binder and other additives. Herein, the binders are improving the adhesion onto the substrate but it makes high electron transfer resistance, which results in slower kinetics and also quasi-reversible or irreversible redox processes [3-4]. To overcome these issues, the SPCEs was subjected to pretreatment with several techniques like chemical, mechanical, vacuum-heat, radiofrequency plasma or laser pretreatment and electrochemical activation. Remarkably, the enhanced electrocatalytic activity with improved electron transfer rate was revealed in the pretreated SPCE. Thus, the pretreatment of SPCEs has considerable attention on the researchers [1-5].

Over the other methods, the electrochemical (EC) activation provides high active sites by means of electrochemical elements and also EC method is low cost and user-friendly. Remarkably, Compton's and Zen's groups have characterized the edge plane and basal plane effects of the electrochemically pre-anodized SPCEs. They claim higher electrocatalytic activity observed in the edge planes when compare to basal planes [6]. Though, SPCEs comprised pyrolytic graphite that encloses both edge planes and basal planes with a ratio that influenced by the quality of the pyrolytic graphite [7]. Furthermore, Zen's group demonstrated the influence of the oxygen moieties in the active edge sites of SPCEs toward the simultaneous determination of biological compounds by the electrochemically pre-anodized SPCE [8]. Following them, we have also reported the chemically activated graphite, electrochemical activated SPCEs for the analytical applications [19,31]. In a progression, we have investigated the electrochemical performance of pretreated SPCEs towards the electro oxidation of acebutolol (ACE).

ACE is a cardio selective, beta-adrenoreceptor blocking agent. This β- blocker ACE drug vastly recommended for the treatment of high blood pressure and arrhythmia of ventricular origin [9]. The drug toxicity caused by the over dosage, which stimulate the adverse effects in human. Therefore, it makes the intense interest on the onsite-monitoring. There are various methods available for the detection of ACE, like chromatography, spectrophotometry, electrophoresis, electrochemical sensor, and spectrofluorimetry [10-15]. Among all, electrochemical process is a suitable one, but it limits their applicability, because of the availability of minimum reports with detailed mechanism for the sensitivity and selectivity of the ACE [16-18,29]. Therefore, we scrutinized the electrochemical detection of ACE on the pretreated SPCEs. These pretreated screen-printed carbon electrode (aSPCE) utilized for the ACE determination, which exhibits the superior electrochemical behavior and good stability.

2. EXPERIMENTAL

2.1. Materials

Acebutolol (ACE), glucose (Glu), uric acid (UA), dopamine (DA), ascorbic acid (AA), glutaric acid (GA), disodium hydrogen phosphate (Na_2HPO_4), sodium dihydrogen phosphate (NaH_2PO_4) and

all other chemicals were acquired from Sigma-Aldrich chemical Co., (USA). The SPCE (working area = 0.07 cm^2) was purchased from Zensor R&D Co., LTD, Taiwan.

2.2. Methods

Cyclic voltammetry (CV) and differential pulse voltammetry (DPV) were performed using CHI 1205 and CHI 900 electrochemical workstations. Raman spectra were recorded using a Raman spectrometer, Dong Woo 500i, Korea, equipped with a charge-coupled detector. Conventional three-electrode system used for the electrochemical experiments where the activated SPCE (aSPCE) used as a working electrode, platinum electrode used as the counter electrode and saturated Ag/AgCl used as a reference electrode.

2.3. Pre-treatment of the SPCE

Prior to the experiments, the SPCE was pre-cleaned with ethanol and water. Then, the SPCEs were activated by sweeping the potential between −0.5 to 2 V for 10 cycles with the scan rate 50 mV/s in a 0.05 M PB (pH 5). After the activation, the SPCEs were gently rinsed with water and dried at room temperature. The activated SPCEs (aSPCEs) were directly applied to the electrochemical studies.

3. RESULTS AND DISCUSSION

3.1. Material characterizations

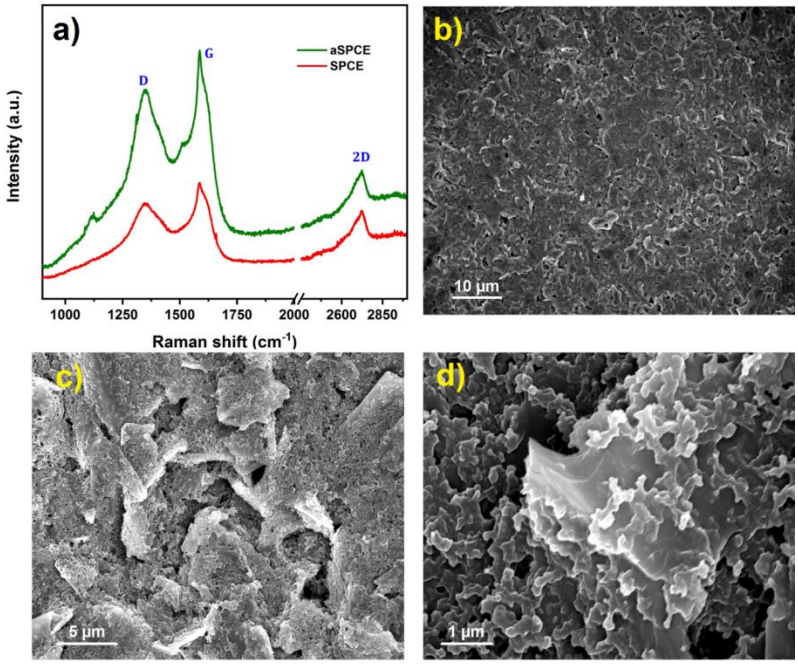

Figure 1. a) Raman spectra of SPCE and aSPCE; b) SEM image of SPCE, c) low and d) high magnification SEM images of aSPCE.

The Raman spectra depict the G band, D band and 2D band of SPCE and aSPCE (Fig.1a). The peaks at 1347 cm^{-1} and 1619 cm^{-1} corresponding to the D band (A_{1g} symmetry) and disordered edges of the graphite, respectively. The peak at 1586 cm^{-1} was attributed to G band (E_{2g} symmetry) of graphite lattice [19-20]. In addition, the 2D overtones peaks are observed at 2722 cm^{-1}; generally, graphene-related materials are characterized by the overtone 2D peak. The intensity ratios (I_{2D}/I_G) have described the exfoliation process or layers of graphene. When compared with SPCE, aSPCE has the higher intensities of D band and G band.

This is because of the introduction of new oxygen functionalities on the SPCE that turn the graphitic basal planes into more active edge planes during the pre-anodization process [19]. Therefore, the intensity and peak shape of the D and G bands of the aSPCE were different [8]. Furthermore, the effect of the pre-anodization process on the local surface was probed by SEM (Fig. 1b-d). The smooth surface depicts in SPCE (Fig. 1b) and the pre anodized surfaces of aSPCE shown in the Fig. 1c & 1d. It can be seen that, the electrochemical activation (itching) makes the corroded like surface on the aSPCE. It increases the roughness of the electrode surface thus the electrochemical active surface area also increased.

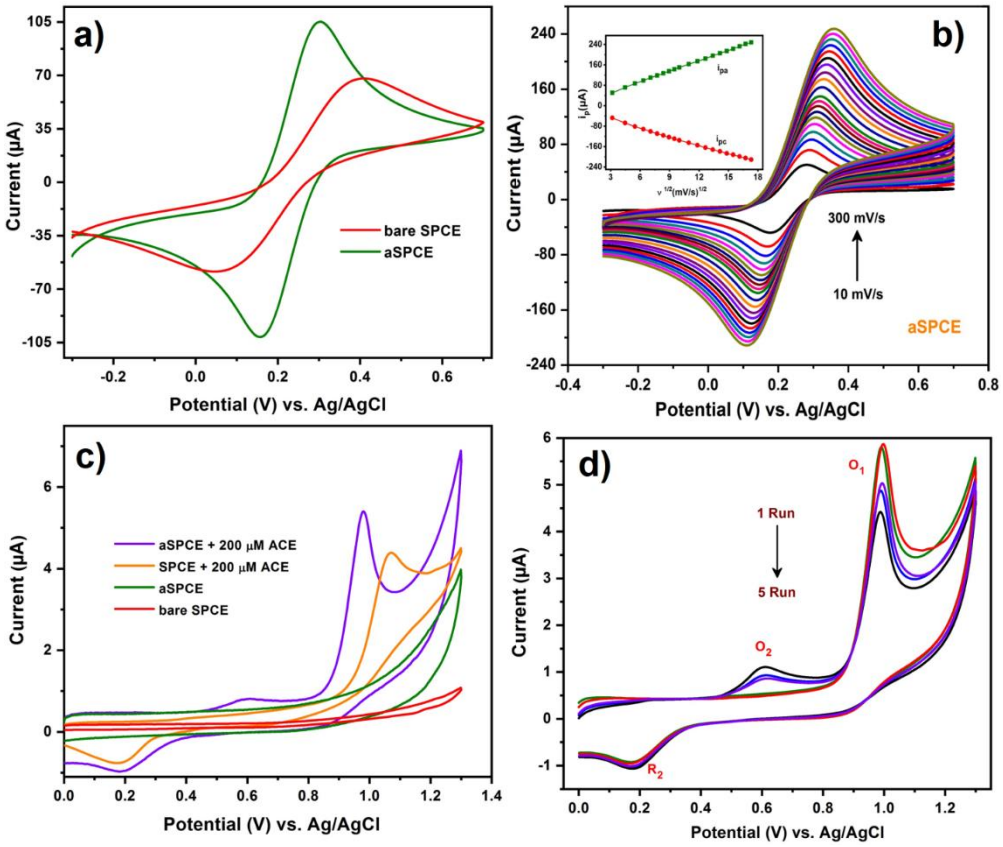

Figure 2. (a) CV responses of bare SPCE and aSPCE in 5 mM $[Fe(CN)_6]^{3/4-}$ system with the supporting electrolyte of 0.1 M KCl (b)The scan rate studies of aSPCE at different scan rates (10 to 300 mV/s) in $[Fe(CN)_6]^{3/4-}$ system (inset; peak current vs $\nu^{1/2}$). (c) The CV response of SPCE and aSPCE electrodes in 0.05 M PB (pH=7) at 50 mV/s in the presence and absence of 200µM ACE. (d) The ACE oxidation on the aSPCE in 1 to 5th run repetitive cycles.

3.2. Electrochemical oxidation of Acebutolol

Before the ACE analysis, the electrochemical behavior of aSPCE was analyzed in the ferricyanide $[Fe(CN)_6]^{3/4-}$ redox probe by the CV technique. This redox probe identifies the active site on the aSPCE with respect to the redox current. Thereby, the electrochemistry of bare SPCE and aSPCE was performed in 0.1 M KCl containing 5mM $[Fe(CN)_6]^{3/4-}$ (Fig.2a). As expected, the characteristic redox couples was observed for the SPCEs that attributed to the redox reaction of $[Fe(CN)_6]^{3/4-}$. The anodic to cathodic peak potential separations ($\Delta E_p = E_{pc} - E_{pa}$) of bare SPCE and aSPCE are revealed as 348 mV and 143 mV respectively (at 50 mV/s scan rate). Herein, the aSPCE displayed a satisfactory ΔE_p when compared to the SPCE. This enhanced performance was obtained by the electrochemical activation because the activation process introduced the electrochemically active elements. Further, the activation process was electrochemically itched the surface of SPCE which creates the active sites (defects). These active sites and active elements are increasing the rate of the reaction. Hence, the aSPCE showed a high redox peak current with less ΔE_p and also it exhibited the good reversible behavior (the redox peak current ratio of bare SPCE and aSPCE shows 0.85, 0.97 respectively) [20]. In addition, the electrochemical active surface area of aSPCE was calculated by using Randles–Sevcik equation [21-22]. The CV studies performed in $[Fe(CN)_6]^{3/4-}$ for the different scan rates (10 to 300 mV/s) and plotted against the $\nu^{1/2}$ (Fig.2b). The Randles–Sevcik equation as follows,

$$i_p = 2.69 \times 10^5 n^{3/2} A C D^{1/2} \nu^{1/2} \quad \ldots\ldots. (1)$$

Where, all the symbols have their meanings as represented in the previous reports [19]. The slopes was plotted against I_{pa} versus $\nu^{1/2}$ (Fig.2b inset) can be used for the electrochemical surface area calculations. The calculated electrochemical surface area of aSPCE and bare SPCE are 0.117, 0.069 cm^2 respectively.

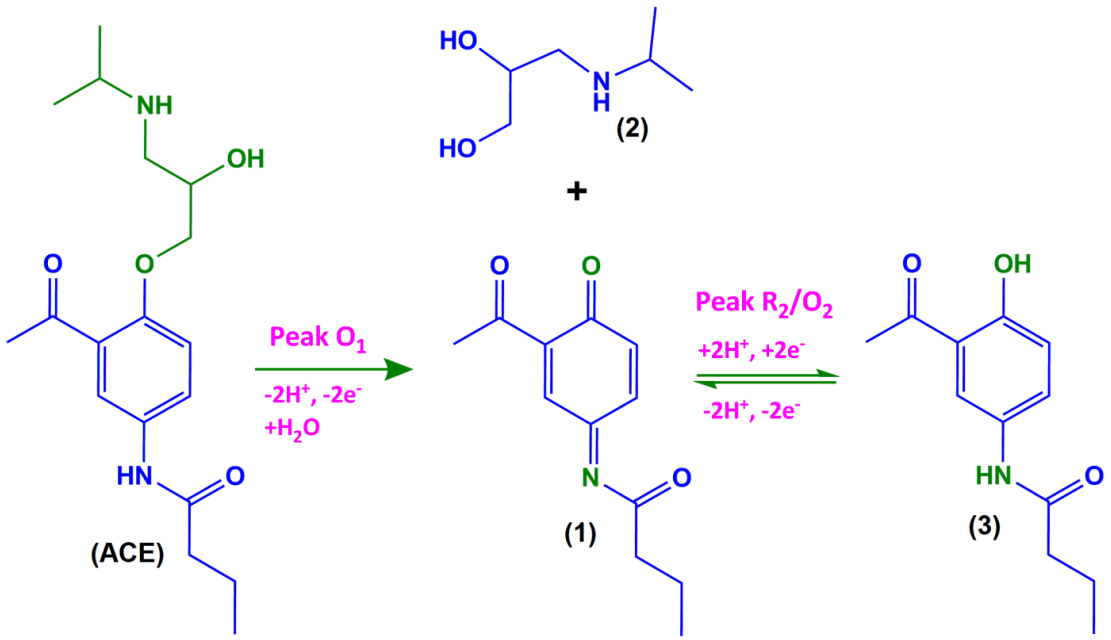

Scheme 1. The schematic illustration of ACE electrochemical oxidation mechanism pathways.

The electrochemical behavior of ACE on modified SPCEs was investigated by CV technique by sweeping the potential from -0.3 V to 0.7 V vs. Ag/AgCl in 0.05 M buffer (pH=7) solution at 50 mV/s scan rate. The CV responses of aSPCE and bare SPCE in the absence and presence of 200 µM ACE was shown in Fig.2c. In the absence of ACE, the bare SPCE shows the low back ground current and aSPCE shows the high current which generally attributed to the double layer capacitance behavior. The high background signal of aSPCE was achieved by the activation process wherein the electrochemically active functional groups are contributed to the charge-discharge properties. In the presence of ACE, both SPCEs revealed the electrocatalytic response for the ACE oxidation (for 200 µM ACE), wherein, aSPCE revealed the high catalytic activity, which exhibits high catalytic peak current (5.4 µA) at low peak potential (0.97V) when compared with bare SPCE. The oxidation of ACE revealed one irreversible oxidation peak (1) and one quasi reversible redox peak (1/3) which observed at +0.96V, +0.6V and +0.186 respectively. The irreversible oxidation peak denotes the conversion of ACE into (*N-(3-acetyl-4-oxocyclohexa-2,5-dienylidene)butyramide*; 1) and (*3-(isopropylamino)propane-1,2-diol*; 2); and then the major oxidized product (1) can be further reduced and formed the (*N-(3-acetyl-4-hydroxyphenyl)butyramide*; 3) at +0.186 V (Scheme. 1) [21-23]. The CV measurement was repeated by several times, in each run the primary oxidation peak current was decreased and redox peak currents were increased. The major oxidation peak O_1 only formed for the ACE oxidation in the 1st run, there is no noticeable other oxidation peaks (Fig.2d). After the fifth run, the CV response of ACE stayed stable. From this experiment, we found the effect of barrier layer adsorption. The primary oxidation product (1) was adsorbed on the surface and limiting the active sites. Thereby, the peak current (O_1) significantly reduced during the repetitive cycles. On the other hand, the redox peak currents were increased. It can be noted that, the reduction peaks (R_2) have only minimal current changes this behavior ensures the adsorptive interface on the electrode surface. In contrast, the bare SPCE-ACE is not showing appreciable oxidation peaks for the ACE. The reason behind this high activity of aSPCE-ACE laid on their electrochemically active functional groups. Therefore, the aSPCE-ACE was used to characterize the further electrochemical studies.

3.3. Effect of scan rate

Fig.3a shows the ACE oxidation response of aSPCE in 200 µM ACE at different scan rates from 10 to 200 mV/s. The major oxidation peak current and redox current were increased gradually while increasing the scan rates. The primary oxidation peak (**1**) was electrocatalytically oxidized the ACE, which controlled by the surface adsorption process (Fig.3a inset). This result endorsed the aforementioned statement about the adsorptive interface on electrode surface. Also, the O_1 peak influences some shift in potential because of the interfacial resistance surface adsorbed products. In addition, the redox reaction controlled by the diffusion wherein the redox products **O_2/R_2** diffused through the adsorptive layer (Fig. 3b) [29]. However, the redox products directly depends on the oxidative products (1) thus if adsorptive layer becomes thicker, the kinetics of the redox products are shuttling.

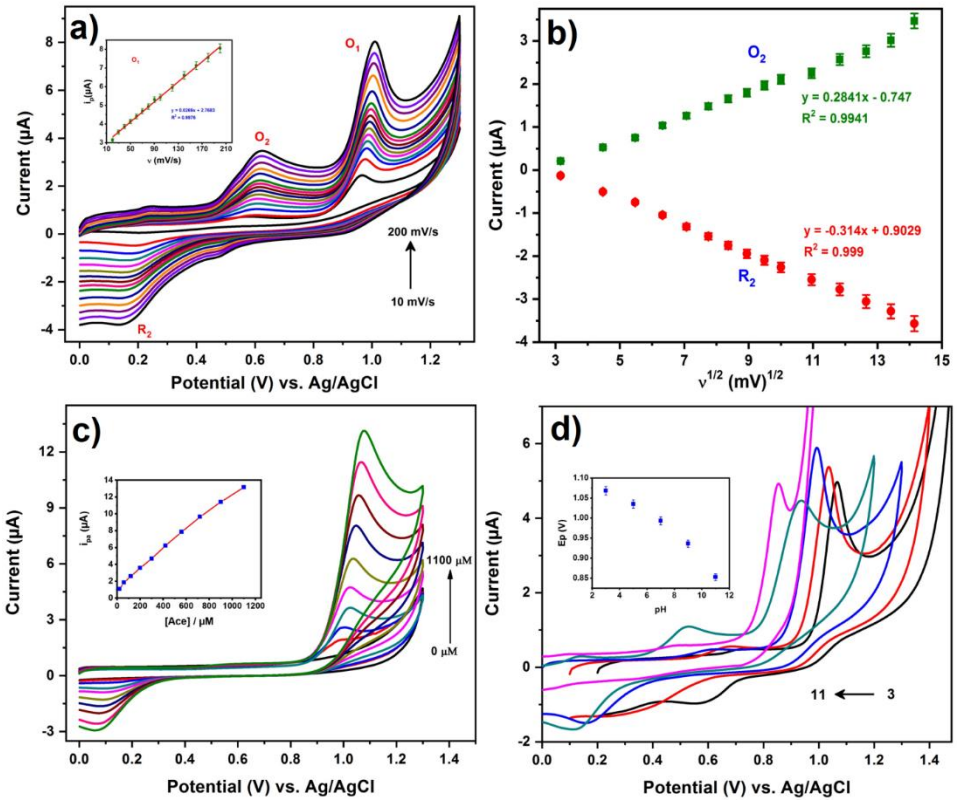

Figure 3. (a) The scan rate studies on aSPCE for the ACE oxidation at different scan rates ranging from 10 to 200 mV/s; inset shows the linear plot of I_{pa} vs ν for the major oxidation peak (O_1). (b) The linear plot between the redox peak currents vs. square root of scan rates. (c) The effect of concentration on the aSPCE towards ACE oxidation by varying the concentrations; inset shows the plot of I_{pa} vs concentrations (d) The ACE oxidation on aSPCE in different pH solutions (pH 3- pH 11); inset shows the plot of the peak potential (O_1) vs. pHs.

Hence, the surface saturation of ACE on the aSPCE was performed by the addition of ACE in the different concentration with the range of 0 to 1100 µM Fig. 3c. The ACE primary oxidation peak current increased while the amount of ACE concentrations increased and the linearity was observed for the peak current and ACE concentrations (Fig. 3c inset).The linearity have deviated from the point where it reaches the saturation thus the surface have an excessive enough active molecules at 900 µM ACE. Noticeably, there is a negligible peak for an oxidation of reduced product (3) however it revealed a strong reduction peak for the product (1); because after the ACE addition we ran only one cycle thus it will not produce the redox couple.

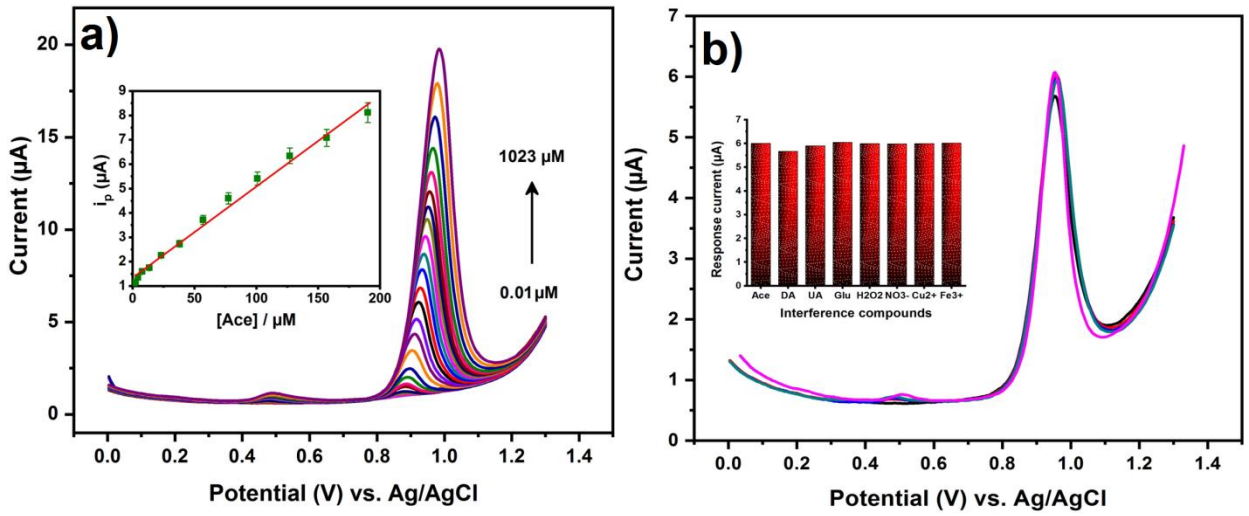

Figure 4. (a) The DPV curves of aSPCE for the ACE oxidation in the different concentrations ranging from 0.01 µM to 1023 µM (inset; plot of I_{pa} vs. different concentrations. (b) Interference studies of ACE with ACE, UA, DA, Glu, H_2O_2, NO_3^-, Cu^{2+}, Fe^{2+}.

3.4. Effect of pH

Fig. 3d showed the CV response of ACE oxidation at aSPCE recorded in various pH solutions (3 to 11) containing 200 µM ACE. In the all pHs, the aSPCE exhibited the well-defined electrochemical response for ACE oxidation. The oxidation peak potential (Epa) was shifted negatively at high pHs. In the high pHs, the nucleophilic interaction ensued in the aromatic benzene group, due to the negative charge of water molecule [16-18, 29-30]. This may reduce the behaviour of the O_2/R_2 products (aminophenol group). Furthermore, peak potential was plotted against the pHs (Fig. 3d inset) which shows the linearity with Epa vs pHs. These results suggested that, the ACE oxidation is fully pH dependent however it showed the slope of about 38 mV/pH. In general, the PCET (proton-coupled electron transfer) employs 59.1mV/pH for the $1e^-$; 1 H^+ transfer. But, the aSPCE revealed 38 mV that manifests the two electron- one proton transfer for the ACE oxidation, results, which does not followed by the single-step process. Hence, this overall electrochemical study states that the oxidation reaction follows a single electron transfer by multi step process on aSPCE.

3.5. Sensitivity and selectivity

Differential pulse voltammetry (DPV) is used to determine the ACE in the 0.05 mM buffer solution (pH 7) solution. Fig. 4a shows the DPV responses of ACE oxidation at aSPCE with varying the concentration of ACE from 0.01 µM to 1023 µM. The oxidation peak current increased with increasing the concentration of ACE. Conversely, the oxidation peak potential was slightly shifted towards positive potential when increasing the concentration which may cause by the more adsorption of high concentration of the analyte between the electrode-electrolyte interfaces. From the DPV studies, we observed the determination of ACE regarding linear concentration and limit of detection (LOD). The ACE primary oxidation peak current was plotted against the concentrations which shown

in the linear plot (Fig. 4a. inset). These results indicates that the primary oxidation peak current (O_1) increased linearly from 0.01 to 200 µM. From the DPV studies, the calculated LOD and sensitivity towards the electrochemical detection of ACE were 0.006 µM and 1.02 µA $\mu M^{-1}cm^{-2}$ respectively. The aSPCE electrochemically oxidized the ACE with significant LOD (6 nM) and satisfactory linear range (0.01 to 200 µM). The performance of the projected material was compared with the peak potential, LOD, linear range and sensitivity of other reported materials (Table 1), which shows the comparable performance with the other reported sensor materials. The tolerance limit and selectivity of the aSPCE was scrutinized in the possible interfering compounds by DPV studies. Most commonly dopamine (DA), uric acid (UA), glucose (Glu) almost has a similar oxidation potential. The two fold excess of UA, DA, Glu, H_2O_2, NO^{3-}, Cu^{2+}, Fe^{2+} interference signals response shown in Fig. 4b. The aSPCE exposed less than 4% interference signals for the ACE oxidation currents. Therefore, the aSPCE can be applicable onsite monitoring for the determination of ACE in practical applications.

Table 1. Comparison of the performance of aSPCE ACE sensor with previously reported ACE sensors.

Method	LOD	Linear range	Ref
EC method / 5H-EGTA/SPCE	0.003 (µM)	0.01-15.1 (µM)	[29]
EC method/Pencil graphite electrode	1.00–15.0 (µM)	0.0126 (µM)	[23]
Mercury drop electrode	168.0 (ng mL^{-1})	168–2016 (ng mL^{-1})	[24]
EC method/Graphene film-GCE	0.131 (ng mL^{-1})	3.36–57.12 (ng mL^{-1})	[25]
EC method/YM NSs/GCE	0.0025 (µM)	0.01–9.6 (µM)	[10]
Spectrophotometric method	46,610 (µg mL^{-1})	5–25 (µg mL^{-1})	[12]
Analytical capillary isotachophoresis	40 (µg mL^{-1})	140–1400 (µg mL^{-1})	[26]
GC-coupled with mass spectroscopy	0.192 (µg mL^{-1})	–	[27]
Electrochemiluminescence	0.0224 (µg mL^{-1})	0.037–186.4 (µg mL^{-1})	[28]
EC method / aSPCE	0.006 (µM)	0.01 to 200 µM	This work

4. CONCLUSIONS

We have reported the practicability of pretreated aSPCE for the determination of ACE. In comparison with bare SPCE, the pretreated SPCE revealed the low peak to peak separation, high electrocatalytic current and low over potential in the electrochemical studies. The scan rate studies and the pH effects have been studied to investigate the mechanisms of ACE oxidation and reaction kinetics on aSPCE. The results showed that the ACE oxidation was mainly preceded through the adsorptive interface reaction. Finally, the aSPCE utilized to the electrochemical determination of ACE which disclosed the acceptable parameters (sensitivity 1.02 µA μM^{-1} cm^{-2}; linear range 0.01 to 200 µM and limit of detection 0.006 µM) and significant interference effects. Therefore, this aSPCE electrode can be applied to the onsite determination of ACE in practical applications.

ACKNOWLEDGMENT
This project was supported by King Saud University, Deanship of Scientific Research, College of Science, Research Center. Also the project was supported by the Ministry of Science and Technology (MOST 107-2113-M-027-005-MY3), Taiwan. This work also jointly supported by the projects from NTUT-NUST-107-1 and NSFC51572126, National Taipei University of Technology and Nanjing University of Science and Technology.

References

1. M. A. T. Gilmartin and J. P. Hart, *Analyst*, 120 (1995) 1029.
2. C. E. Banks and R. G. Compton, *Analyst*, 131 (2006) 15.
3. J.Wang, M.Pedrero, H.Sakslund, O.Hammerich and J.Pingarron, *Analyst*, 121(1996) 345-350.
4. H. Wei, J. J. Sun, Y. Xie, C. G. Lin, Y. M. Wang, W. H. Yin and G. N. Chen, *Anal. Chim. Acta*, 588 (2007) 297.
5. J. F. Evans and T. Kuwana, *Anal. Chem*., 51(1979) 358.
6. F. Wantz, C. E. Banks, and R. G. Compton, *Electroanalysis*, 17 (2005) 1529.
7. R. T. Kachoosangi,C. E.Banks, and R. G. Compton, *Electroanalysis*, 18 (2006) 741.
8. K. S. Prasad,G.Muthuraman, and J. M. Zen, *Electrochem. Commun.*, 10 (2008) 559.
9. M. Sabidó, H. Thilo, G. Guido, *Pharmacol. Res*., 139 (2019) 106–112.
10. T.-W. Chen, J.V. Kumar, S.-M. Chen, B. Mutharani, R. Karthik, E.R. Nagarajan, V.Muthuraj, *Chem. Eng.J*., 359 (2019) 1472–1485.
11. D.H. Manjunatha, S.M.T. Shaikh, K. Harikrishna, R. Sudhirkumar, P.B. Kandagal, J. Seetharamappa, *Eclet. Quim*., 33 (2008) 37–40.
12. H.E. Abdellatef, M.M. El-Henawee, H.M. El-Sayed, M.M. Ayad, *Spectrochim. Acta Part A Mol. Biomol. Spectrosc.*, 65 (2006) 1087–1092.
13. A. El-Gindy, A. Ashour, L. Abdel-Fattah, M.M. Shabana, *J. Pharm. Biomed. Anal.*, 24 (2001) 527–534.
14. P. V. Meffin, S.R. Harapat, Y.-G. Yee, D.C. Harrison, *J. Chromatogr., A*.138 (1977)183–191.
15. G. A. Forbes, T.A. Nieman, J. V Sweedler, *Anal. Chim. Acta*, 347 (1997) 289–293.
16. U. Bussy, V. Ferchaud-Roucher, I. Tea, M. Krempf, V. Silvestre, M. Boujtita, *Electrochim. Acta*, 69 (2012) 351–357.
17. U. Bussy, I. Tea, V. Ferchaud-Roucher, M. Krempf, V. Silvestre, N. Galland, D. Jacquemin, M. Andresen-Bergström, U. Jurva, M. Boujtita, *Anal. Chim. Acta*, 762 (2013) 39–46.
18. U. Bussy, U. Jurva, R. Boisseau, M. Andresen Bergström, V. Silvestre, N. Galland, D. Jacquemin, M. Boujtita, *Rapid Commun. Mass Spectrom.,* 29 (2015) 456–460
19. N. Karikalan, P. Sundaresan, S. M. Chen, and R. Karthik, *J. Electrochem. Soc*, 165 (14) (2018) H969 - H978.
20. N. Karikalan, R. Karthik, S. M. Chen, M. Velmurugan, and C. Karuppiah, *J. Colloid Interface. Sci*., 483 (2016) 109.
21. N. Karikalan, R. Karthik, S.M. Chen, H.A. Chen, *Sci. Rep*., 7 (2017)
22. M. Velmurugan, N. Karikalan, S.M. Chen, Y.H. Cheng, C. Karuppiah, *J. Colloid. Interface Sci*., 500 (2017) 54–62.
23. A.M. Bagoji, S.M. Patil, S.T. Nandibewoor*, Cogent Chem*., 2 (2016) 1172393.
24. A. F. Al-Ghamdi, M. M. Hefnawy, A. A. Al-Majed and F. F. Belal, *Chem. Cent. J*., 2012, 6, 15–22.
25. A.M. Bagoji, S.T. Nandibewoor, *New J. Chem*., 40 (2016) 3763–3772.
26. M. Pospíšilová, A. Kavalírová, M. Polášek, *J. Chromatogr. A*., 1081 (2005) 72–76.
27. E. Pujos, C. Cren-Olivé, O. Paisse, M.-M. Flament-Waton, M.-F. Grenier-Loustalot, *J. Chromatogr. B*. 877 (2009) 4007–4014

28. X. Li, D. Zhu, T. You, *Electrophoresis*, 32 (2011) 2139–2147.
29. N. Karikalan, M. Elavarasan, T.C.K. Yang, *Ultrason. Sonochem*, 56 (2019) 297-304.
30. M. Moradi, M. Moazeni, H.R. Salimijazi, *Vacuum*, 107 (2014) 34–40.
31. N. Karikalan, S. Kubendhiran, S.M. Chen, P. Sundaresan, R. Karthik, *J. Catal*, 356 (2017), 43-52.